Thermochimica Acta, 103 (1986) 305–316
Elsevier Science Publishers B.V., Amsterdam – Printed in The Netherlands

THERMAL STUDIES ON PURINE COMPLEXES. XII. THERMAL BEHAVIOUR OF SOME METAL COMPLEXES OF HYPOXANTHINE

M. QUIRÓS OLAZÁBAL, J.M. SALAS PEREGRÍN * and M.P. SÁNCHEZ SÁNCHEZ
Department of Inorganic Chemistry, Faculty of Sciences, University of Granada, 18071-Granada (Spain)

F. GIRELA VILCHEZ and M. ROLDÁN MEDINA
Estación Experimental Zaidin, C.S.I.C., Granada (Spain)

(Received 12 December 1985)

ABSTRACT

Some complexes of hypoxanthine with Cu(II), Ag(I), Cd(II), Hg(II), Pd(II), Rh(III) and Pt(IV) have been prepared in ethanolic, aqueous, basic or acid media and characterized on the basis of elemental analysis and IR studies. The thermal behaviour of these compounds has been studied using TG, DTG and DSC techniques. Heats of dehydration, dehalogenation and fusion have been calculated from DSC curves.

INTRODUCTION

The hypoxanthine ring is a very important structure in purine nucleotide biochemistry since adenine and guanine rings arise from it in living things [1].

Hypoxanthine can exist in aqueous solution in four possible forms, depending on pH: protonated, molecular, monoanionic and dianionic. In this paper hypoxanthine compounds of each of these four forms have been isolated.

Some of them have been described previously in the literature [2–9], but we have found no references about their thermal behaviour. For this reason and following our studies on purine complexes [10–17], in the present paper the thermal behaviour of some hypoxanthine complexes is described.

---

* To whom all the correspondence should be addressed.

EXPERIMENTAL

Materials

Hypoxanthine (6-hydroxy-purine) was purchased from E. Merck. All the inorganic products used were of analytical reagent grade.

Methods

Microanalysis of C, H and N were carried out in a Carlo Erba microanalyzer model 1106; determination of metal ions was carried out gravimetrically.

The IR spectra of the compounds were recorded in KBr pellets in the 4000–200 cm^{-1} region using a Beckman 4250 spectrophotometer.

TG studies were made using a dynamic atmosphere of pure air with a flow rate of 100 ml min^{-1} on a Mettler thermobalance model TG-50 at a heating rate of 20°C min^{-1}. The DSC curves were recorded in a Mettler differential scanning calorimeter model DSC-20 at a heating rate of 10°C min^{-1}, in the temperature range 35–500°C.

The thermolytic reactions were carried out with samples varying in weight from 1.7 to 13.5 mg.

Preparation of the complexes

All compounds were prepared by mixing two solutions: one of them (100 ml) containing 2.2×10^{-3} moles of hypoxanthine (or its chlorohydrate, in the case of $CuHxCl_2$ and $CuHxBr_2 \cdot 1/2H_2O$) and the other one containing the necessary amount of metal ions so that the metal:ligand ratios were 1 : 2.

Metal chlorides were employed as inorganic salts in every case except for silver complexes and $CuHxBr_2 \cdot 1/2H_2O$ where silver nitrate and copper bromide, respectively, were used.

The resultant solutions were refluxed (30 min) with continuous stirring.

After a variable time precipitates appeared which were filtered, washed consecutively with water and ethanol and dried with ether. The complex Hg(Hx)Cl was obtained from the mother liquor of $Hg(Hx)_2Cl_2 \cdot H_2O$.

Reaction media, analytical data and colours of the isolated compounds are presented in Table 1.

RESULTS AND DISCUSSION

The IR data of the isolated compounds are tabulated in Table 2. These data agree with the protonated, molecular, monoanionic or dianionic actuation of hypoxanthine suggested by elemental analysis.

TABLE 1

Chemical analysis of the compounds

Complex	Reaction medium	Colour	%C		%H		%N		% Metal	
			found	calc.	found	calc.	found	calc.	found	calc.
$Cu(Hx)_2Cl_2 \cdot 1/2H_2O$	water	blue	28.69	28.86	1.48	2.16	26.15	26.93	15.8	15.29
$Cu(Hx)Cl$	ethanol	greenish yellow	23.85	22.18	1.59	1.48	21.09	20.70	24.8	23.49
$Cu(Hx)Br_2 \cdot 1/2H_2O$	ethanol	brown	16.86	16.28	2.18	1.36	14.57	15.20	16.6	17.24
$Ag(Hx)NO_3$	HNO_3 1:1	white	19.94	19.61	1.26	1.31	22.05	22.88	36.3	35.25
Ag_2Hx	NH_3 1:1	white	17.29	17.15	0.59	0.57	15.72	16.01	61.8	61.67
$Hg(Hx)_2Cl_2 \cdot H_2O$	water	white	22.66	21.38	1.63	1.78	20.86	19.94	–	35.71
$Hg(Hx)Cl$	water	white	16.99	16.16	1.07	0.81	15.20	15.09	–	54.05
$Pd(Hx)Cl_2$	water	yellow	19.94	19.14	1.63	1.27	17.94	17.87	34.0	33.94
$Rh(Hx)_2Cl_3$	water	yellow	23.85	24.92	1.82	1.66	22.10	23.26	21.9	21.37
$(HxH)_2(PtCl_6)$	HCl 1:1	reddish brown	17.99	17.59	1.56	1.47	16.34	16.42	28.0	28.60

TABLE 2

Infrared data for the compounds (all values are in cm^{-1})

Compound	ν(O–H)	ν(N–H)	ν(C–H)	ν(C=O)	ν(C=N)+ν(C=C)	$\nu(NO_3^-)$	ν(C–N)	ν(C–O)
Hypoxanthine	–	3120, 3040	2910, 2810	1665	1575	–	1340, 1265, 1205	–
Hypoxanthine chlorhydrate	3395	3120–2700	2940, 2840	1670	1615, 1570	–	1370, 1305, 1250	–
$Cu(Hx)_2Cl_2 \cdot 1/2H_2O$	3520, 3460	3130, 3080	2920, 2840	1670	1590, 1530	–	1320, 1250, 1175	–
$Cu(Hx)Cl_2$	–	3080, 3040	2880, 2810	1700	1580	–	1395, 1205	–
$Cu(Hx)Br_2 \cdot 1/2H_2O$	3530, 3490	3120, 3040	2890, 2820	1705	1600, 1540	–	1390, 1210	–
$Ag(Hx)NO_3$	–	3120, 3040	2910, 2810	1665	1575	1375	1340, 1265, 1205	–
$Ag_2(Hx)$	–	–	2820	–	1620	–	1330, 1270, 1210	1100
$Hg(Hx)_2Cl_2 \cdot H_2O$	3560, 3510	3090, 3040	2910, 2800	1665	1570	–	1365, 1300, 1205	–
$Hg(Hx)Cl$	–	3110	2910, 2840	1675	1580, 1545	–	1360, 1330, 1170	–
$Pd(Hx)Cl_2$	–	3105	2900	1690	1585, 1540	–	1405, 1330, 1180	–
$Rh(Hx)_2Cl_3$	–	3120	2900	1670	1585	–	1390, 1325, 1190	–
$(HxH)_2(PtCl_6)$	–	3300–2700	2940, 2840	1670	1620, 1580	–	1375, 1310, 1250	–

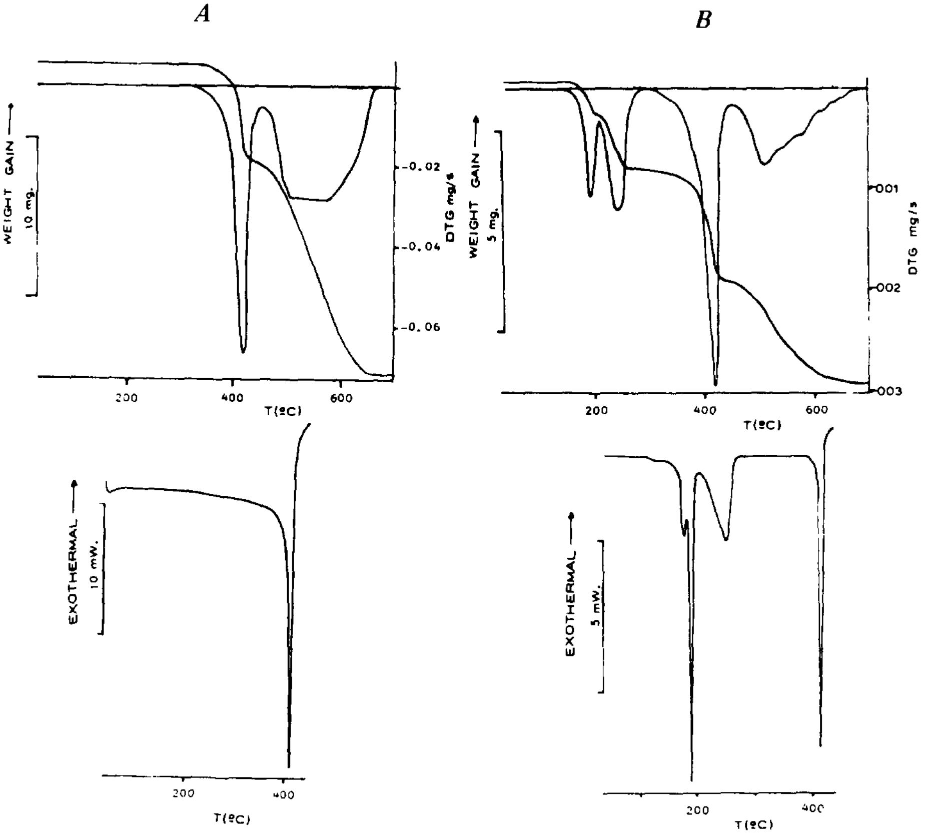

Fig. 1. TG and DSC curves of: (A) hypoxanthine and (B) its chlorhydrate.

Thus, in the IR spectrum of $(HxH)_2(PtCl_6)$, the bands corresponding to ν(C=C) and ν(C=N) stretching vibrations appear at higher wavenumber with respect to their position in the free ligand spectrum. This fact is due, according to the literature, to a protonation process in the imidazole ring [18].

The $Ag_2(Hx)$ spectrum shows a new band at 1100 cm^{-1}, assigned to ν(C–O) of the dianionic form of hypoxanthine.

On the other hand, the IR spectrum of Hg(Hx)Cl shows a decrease in the number of bands corresponding to ν(N–H) with respect to the spectrum of free hypoxanthine. This may be due to the partial deprotonation of the ligand in this compound.

The remaining complexes present an IR spectrum which suggests that coordination of hypoxanthine base to metal ions takes place in molecular form.

TG and DSC curves of the compounds are shown in Figs. 1–4.

Four different processes can be observed in these diagrams: dehydration, dehalogenation, fusion and pyrolysis.

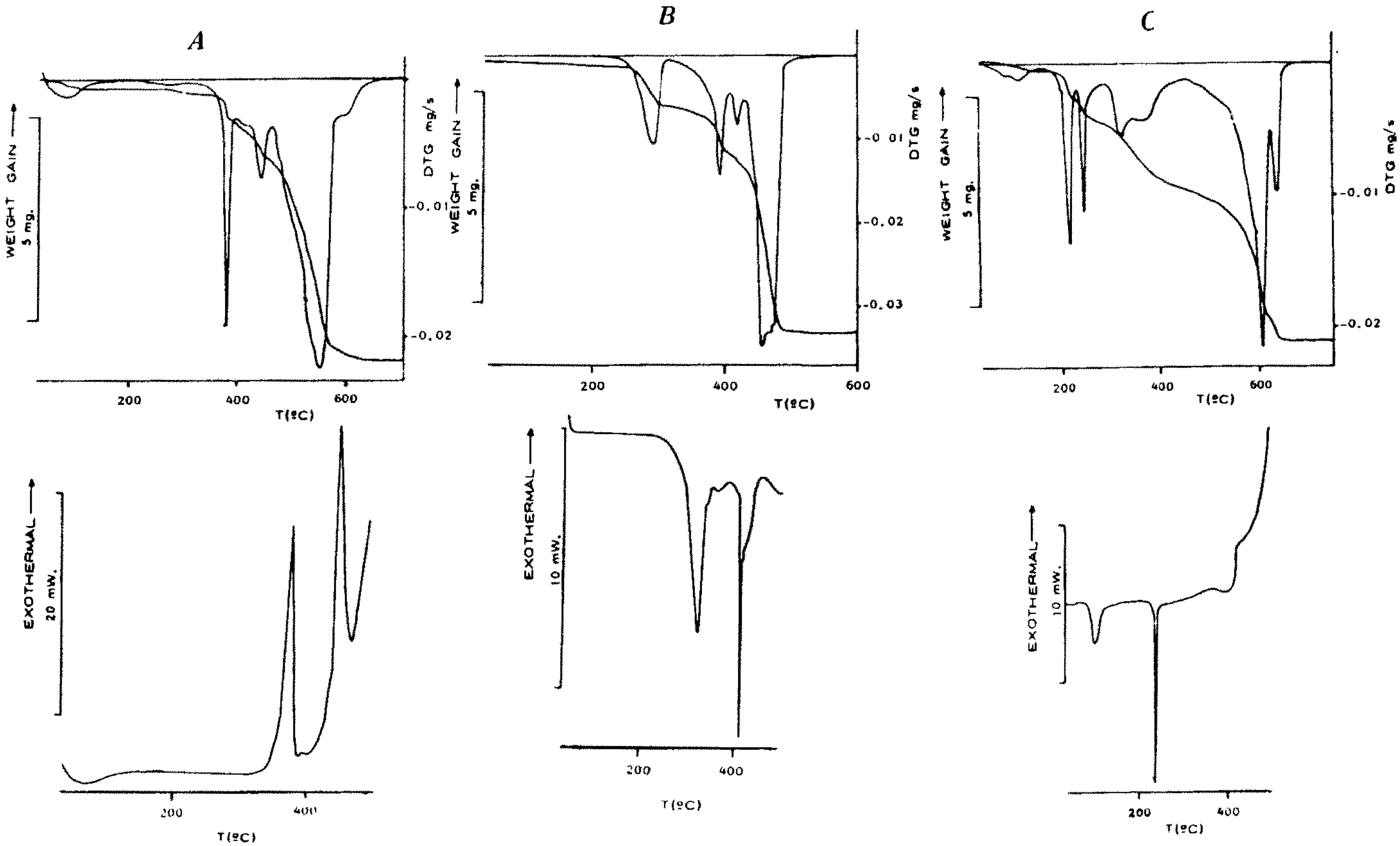

Fig. 2. TG and DSC curves of: (A) $Cu(Hx)_2Cl_2{\cdot}1/2H_2O$; (B) $Cu(Hx)Cl_2$ and (C) $Cu(Hx)Br_2.\ 1/2H_2O$.

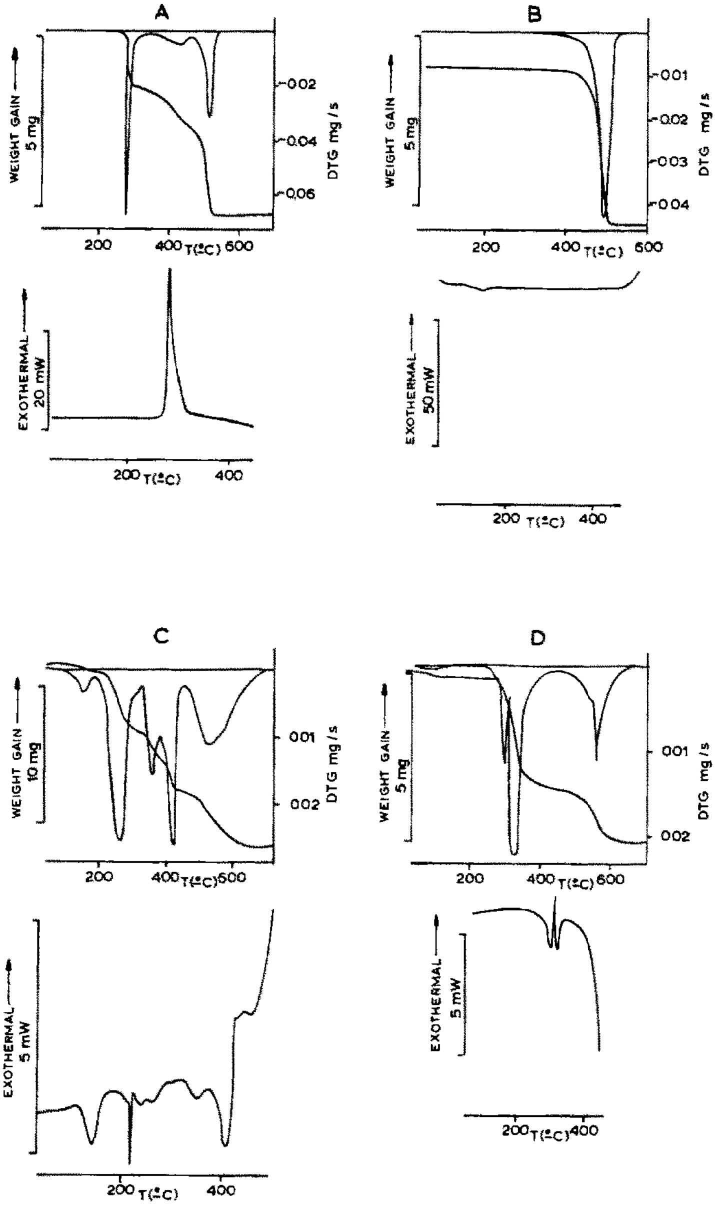

Fig. 3. TG and DSC curves of: (A) $Ag(Hx)NO_3$; (B) Ag_2Hx; (C) $Hg(Hx)_2Cl_2 \cdot H_2O$ and (D) $Hg(Hx)Cl$.

Dehydration processes

The first step of thermal decomposition of hydrated compounds is the elimination of water. Corresponding data for these processes are given in Table 3.

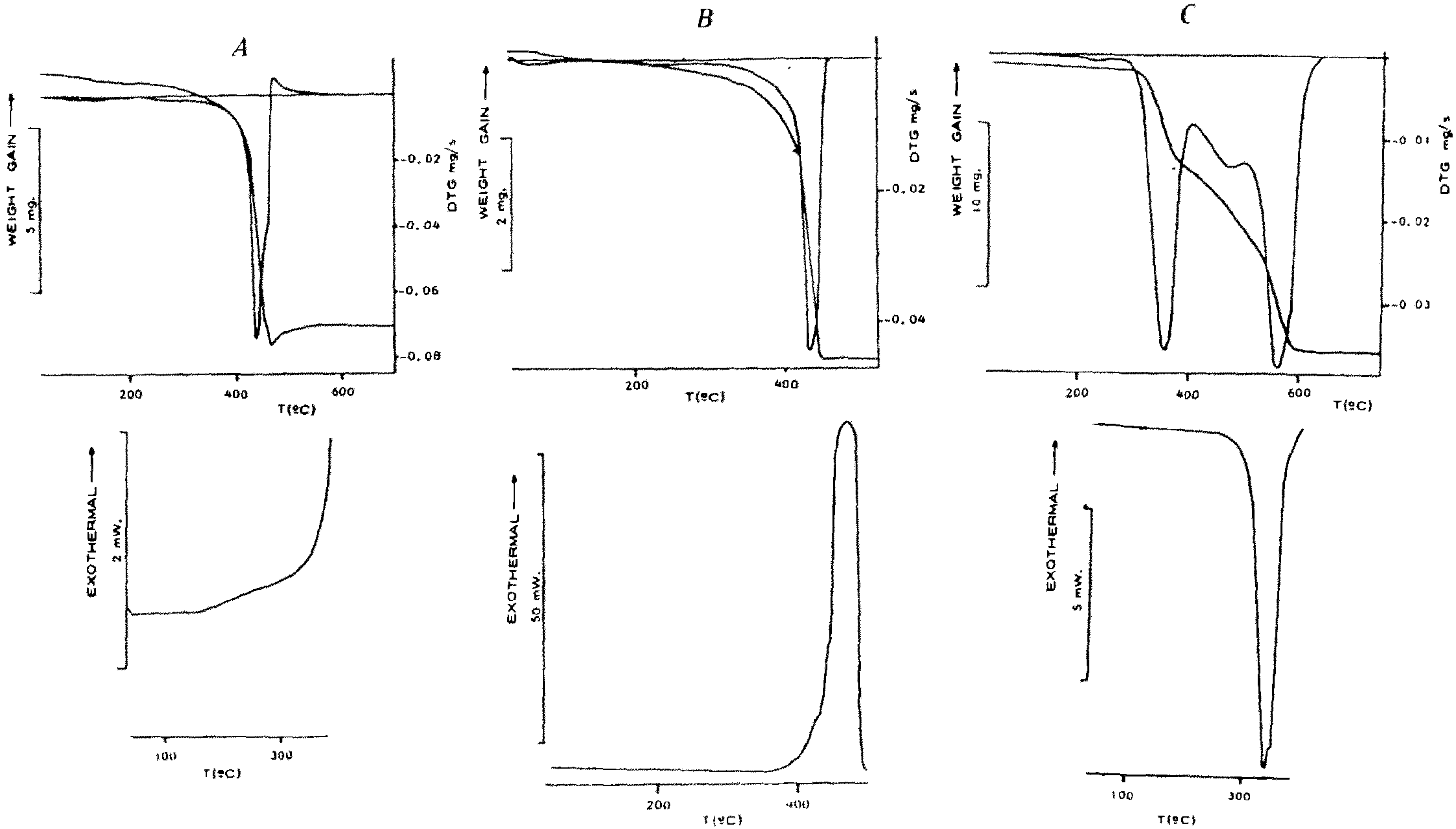

Fig. 4. TG and DSC curves of: (A) $Pd(Hx)Cl_2$; (B) $Rh(Hx)_2Cl_3$ and (C) $(HxH)_2(PtCl_6)$.

TABLE 3

Thermoanalytical data for dehydration processes

Compound	Weight loss (%) calc.	Weight loss (%) obs.	Temperature range (°C)	Peak temperature DSC (°C)	Dehydration enthalpy (kJ (mol $H_2O)^{-1}$)
$(HxH)Cl \cdot H_2O$	9.44	10.2	160–220	189	52.4
$Cu(Hx)_2Cl_2 \cdot 1/2H_2O$	2.16	2.7	40–120	80	
$Cu(Hx)Br_2 \cdot 1/2H_2O$	2.44	2.7	50–140	100	71.4
$Hg(Hx)_2Cl_2 \cdot H_2O$	3.20	3.7	100–180	140	43.8

Dehydration of these compounds occurs in one single step, over a variable temperature range. Weight losses observed in TG curves are in agreement with those calculated from the proposed formulas.

The expected endothermic behaviour for such processes has been observed in DSC curves in the same temperature range. The corresponding dehydration enthalpies and temperature peaks are also given in Table 3.

Dehydration enthalpy values are fairly high. This suggests a very strong interaction between water molecules and hypoxanthine.

Dehalogenation processes

Data corresponding to the dehalogenation of halogenated compounds are shown in Table 4.

A very important feature is observed in the DTG curve of the three copper complexes (Fig. 2): the elimination of the halogen atoms is not simultaneous. This suggests that these atoms are not equivalent.

The crystal structure of the complex $Cu(Hx)_2Cl_2 \cdot 3H_2O$ was solved by Sletten [4] using X-ray diffraction methods. This study shows that only one of the chlorine atoms is directly coordinated to the copper ion, which agrees with our thermoanalytical data.

A dimeric structure has been proposed for the complexes $Cu(Hx)Cl_2$ and $Cu(Hx)Br_2 \cdot 1/2H_2O$. In such a structure there are two structurally different types of halogen atoms: terminal and bridging. This also agrees with DTG data.

In mercury complexes (Fig. 3), chlorine and mercury are eliminated simultaneously. This process corresponds with endothermic effects in their DSC diagrams.

The dehalogenation processes of $Pd(Hx)Cl_2$ and $Rh(Hx)_2Cl_3$ (Fig. 4) overlap with the pyrolytic process of the purine ring, and suggest very strong bonds palladium–chlorine and rhodium–chlorine.

Finally, in the complex $(HxH)_2(PtCl_6)$ (Fig. 4), a dehalogenation process could take place with the loss of two moles of hydrogen chloride and two

TABLE 4

Thermoanalytical data for dehalogenation processes

Compound	Eliminated species	Accumulated weight		Temperature range (°C)	Peak temperature (DSC)	Total ΔH (kJ mol^{-1})
		calc.	obs.			
(HxH)Cl·H_2O	HCl	28.64	28.4	210–260	250	51.5
Cu(Hx)$_2$Cl$_2$·1/2H_2O	1/2Cl_2	10.69	11.9	350–400	[a]	[a]
	1/2Cl_2	19.24	20.3	400–460	[a]	[a]
Cu(Hx)Cl_2	1/2Cl_2	13.10	11.9	235–320	318	107
	1/2Cl_2	26.20	24.5	350–410	[a]	[a]
Cu(Hx)Br_2·1/2H_2O	1/2Br_2	24.62	24.2	200–290	[a]	[a]
	1/2Br_2	45.81	44.6	290–450	[a]	[a]
Hg(Hx)$_2$Cl$_2$·H_2O	HgCl_2	51.53	50.4	180–370	237 and 343	Not integrated
Hg(Hx)Cl	Hg+1/2Cl_2	63.60	64.3	250–410	294 and 310	58.9
Pd(Hx)Cl_2	Cl_2	22.62	[a]	[a]	[a]	[a]
Rh(Hx)$_2$Cl$_3$	3/2Cl_2	30.79	[a]	[a]	[a]	[a]
(HxH)$_2$(PtCl_6)	2HCl+2Cl_2	31.48	30.6	280–410	339	246

[a] Overlapping with pyrolysis.

moles of chlorine per mole of initial compound. This fact has been confirmed from IR spectroscopy in other analogous compounds [19]. However, we cannot isolate the intermediate compound because of the overlapping of dehalogenation and pyrolytic processes.

Melting processes

The DSC diagram of hypoxanthine (Fig. 1) shows an endothermic effect centered at 410°C, just before pyrolytic decomposition. This effect has been assigned to the fusion of the purine base. The fusion enthalpy, calculated from the peak area is 29.2 kJ mol^{-1}. This value is similar to those of other purine bases [16,20].

The DSC diagram of hypoxanthine chlorhydrate (Fig. 1) and those of $Hg(Hx)_2Cl_2 \cdot H_2O$ and Hg(Hx)Cl (Fig. 3) show a similar feature. This occurs because the result of dehydration and dehalogenation of these compounds is merely hypoxanthine.

The DSC diagram of $Cu(Hx)Cl_2$ (Fig. 2) also shows an acute endothermic peak at 413°C, with an associated enthalpy of 28.4 kJ mol^{-1}. This effect has been assigned to the fusion of the intermediate compound.

Finally, the anhydrous $Cu(Hx)Br_2$ and $Hg(Hx)_2Cl_2$ melt at 236 and 219°C, with fusion enthalpies of 36.2 and 9.7 kJ mol^{-1}, respectively.

Pyrolytic processes

Thermogravimetric data for pyrolytic processes are shown in Table 5. All dehydrated and dehalogenated compounds show exothermic effects in their

TABLE 5

Thermoanalytical data for pyrolytic processes

Compound	Temperature range	DSC peak temperature	Nature	Residue	
				% found	% calc.
Hx	360–549	> 500	–	–	–
$(HxH)Cl \cdot H_2O$	360–540	> 500	–	–	–
$Cu(Hx)_2Cl_2 \cdot 1/2H_2O$	460–600	382, 455, > 500	CuO	20.2	19.10
$Cu(Hx)Cl_2$	410–500	> 450	CuO	31.0	29.40
$Cu(Hx)Br_2 \cdot 1/2H_2O$	450–660	> 500	Cu	16.6	17.24
$Ag(Hx)NO_3$	255–300	269	Ag	36.3	35.25
	370–530	> 450			
$Ag_2(Hx)$	390–530	> 450	Ag	61.8	61.67
$Hg(Hx)_2Cl_2 \cdot H_2O$	370–650	> 500	–	–	–
Hg(Hx)Cl	410–650	> 500	–	–	–
$Pd(Hx)Cl_2$	250–550 [a]	> 400	PdO	39.1	39.05
$Rh(Hx)_2Cl_3$	300–470 [a]	470	Rh_2O_3	27.0	26.36
$(HxH)_2(PtCl_6)$	410–600	> 400	Pt	28.0	28.60

[a] Includes dehalogenation.

DSC curves, which are attributed to the combustion of organic matter. In the cases of palladium and rhodium complexes, the dehalogenation process is included in the pyrolytic process.

The DSC diagram of $Ag(Hx)NO_3$ also shows an exothermic effect, centered at 269°C, due to the pyrolysis of nitrate ion. After this, combustion of organic matter takes place.

The pyrolysis residues are also given in Table 5. The resulting metal or oxide was identified by infrared spectroscopy. Experimental values are in good agreement with theoretically expected ones.

REFERENCES

1 A.L. Lehninger, Bioquímica: Las Bases Moleculares de la Estructura y Función Celular, 6th edn., Omega, Barcelona, 1980.
2 R. Weiss and H. Venner, Z. Physiol. Chem., 340 (3–4) (1965) 138.
3 R. Weiss and H. Venner, Z. Chem., 7 (11) (1967) 428.
4 E. Sletten, Acta Crystallogr. B, 26 (1970) 1609.
5 T. Asakawa, M. Inone, K. Hara and M. Kubo, Bull. Chem. Soc. Jpn., 15 (1972) 1054.
6 M.R. Caira, L.R. Nassimbeni and A.L. Rodgers, Acta Crystallogr., Sect. B, 31 (4), (1975) 1112.
7 M.J. Clarke, Inorg. Chem., 16 (4) (1977) 738.
8 M.E. Kastner, K.F. Coffey, S.E. Edmonds and K. Eriks, J. Am. Chem. Soc., 103 (1981) 5747.
9 Ch. M. Mikulski, T.B. Tran and L. Mattucci, Inorg. Chim. Acta, 78 (1983) 211.
10 J.M. Salas Peregrín, E. Colacio Rodríguez, J.D. López González and C. Valenzuela Calahorro, Thermochim. Acta, 63 (1983) 145.
11 E. Colacio Rodríguez, J.M. Salas Peregrín, M.P. Sánchez Sánchez and A. Mata Arjona, Thermochim. Acta, 66 (1983) 245.
12 J.M. Salas Peregrín, E. Colacio Rodríguez, M.A. Romero Molina and M.P. Sánchez Sánchez, Thermochim. Acta, 69 (1983) 313.
13 E. Colacio Rodríguez, J.M. Salas Peregrín, R. López Garzón and J.D. López González, Thermochim. Acta, 71 (1983) 139.
14 E. Colacio Rodríguez and J.M. Salas Peregrín, Thermochim. Acta, 74 (1984) 45.
15 E. Colacio Rodríguez, J.M. Salas Peregrín, M.A. Romero Molina and R. López Garzón, Thermochim. Acta, 76 (1984) 373.
16 J.M. Salas Peregrín, E. Colacio Rodríguez, F. Girela Vilchez and M. Roldán Medina, Thermochim. Acta, 80 (1984) 323.
17 E. Colacio Rodríguez, J.D. López González and J.M. Salas Peregrín, J. Thermal Anal., 28 (1983) 3.
18 W. Adam, A. Grimison and Q. Rodríguez, Tetrahedron, 23 (1967) 2513.
19 M. Moreno Carretero, E. Colacio Rodríguez and J.M. Salas Peregrín, Thermochim. Acta, 93 (1985) 73.
20 J.H. Speer and A.L. Raymond, J. Am. Chem. Soc., 75 (1953) 114.